

A NUMERICAL AND EXPERIMENTAL STUDY IN RESISTANCE SPOT WELDING PROCESS

Chainarong SRIKUNWONG[†], Thomas DUPUY^{††}
and Yves BIENVENU[†]

[†]Centre des Matériaux P-M. Fourt, Ecole des Mines de Paris, F-91003, Evry cedex, France
Phone: 33-160763035 Fax: 33-160763150

E-mail: DK.SRIKUNWO@ARCELOR.COM, Yves.Bienvenu@mat.ensmp.fr

^{††}CRDM, Arcelor Group, F-59381, Dunkerque cedex 1, France

Phone: 33-328293387 Fax: 33-328296429

E-mail: thomas.dupuy@arcelor.com

ABSTRACT:

In the present study, 2-D axisymmetric finite element models incorporating with electrical-thermal and thermal-mechanical coupling procedures were applied to simulate the resistance spot welding (RSW) process. The temperature dependency characteristics and properties of both sheets and electrodes were included in the model. The experimental study and validation were carried out for nugget formation at the upper limits of weldability lobe. The validation in terms of nugget development was conducted in the case of joining sheets with curved-face electrode. The influence of electrical-thermal data input variability were comprehensively investigated and underlined in the study. The results of electrical-thermal analysis were discussed with the view of thermal history investigation during RSW process.

1. INTRODUCTION:

Benefits of its process advantages including joining performance, flexibility, robustness and hi-speed of process with very high quality joints at very low cost, RSW has found to be a major joining technique utilized for automotive assembly fabrication. However, due to a very short operation time being commonly less than one second, it is not therefore an easy task to assess or disclose entirely the internal process characteristics by practical means when the variability of welding parameters or that of sheet configurations is encountered.

Numerical modeling can be therefore considered as another approach to obtain a better understanding in process characteristics and consequently helps improving the joining quality as well as process performance.

There has been a great deal of effort devoted to RSW simulation development documented in literature¹⁻⁴. Both decoupled and coupled techniques have been commonly implemented to analyze the process mechanisms, which are associated with electrical, thermal, and mechanical interactions. Not only the nugget formation or the thermal history occurring in the weld but also the thermal induced stresses can be considered as the features of coupled analysis.

2. EXPERIMENTAL RESULTS AND DISCUSSION:

Weld Geometry Development Mechanisms in Stackup and Heavy Gauge Sheet Joinings-A review:

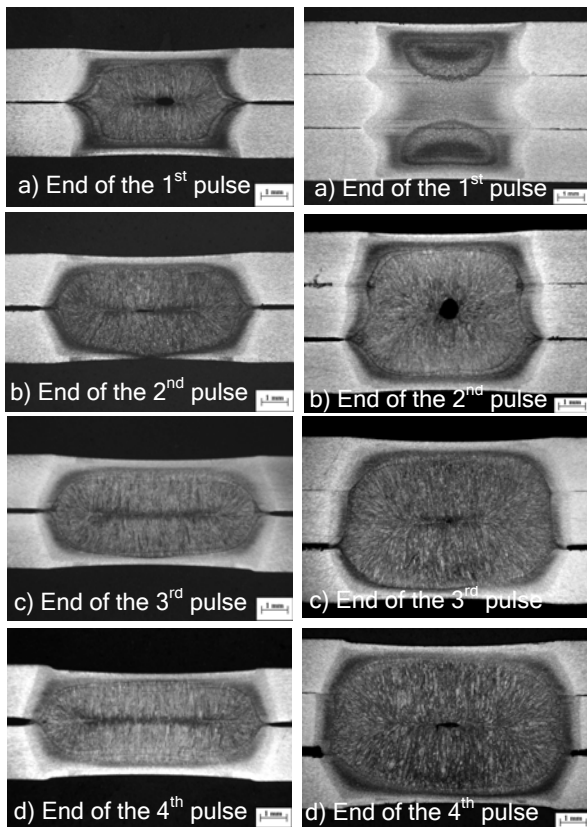
Welding schedules utilized in the study are prior given from ISO 18278-2/2003 with the application of curved-faced electrodes of 6- and 8-mm diameter, namely TH6 and TH8 respectively. The pedestal spot welding machine used and signal monitoring setup for welding operation are shown in Fig. 1.

Macro-photographs of nugget development kinetics in the case of two- and three-sheet heavy gauge joining at the end of each interrupted pulse are displayed in Fig. 2. The nugget develops progressively until the end of welding for both cases. In case of three-sheet joining, the hot zone originates in the upper and the lower regions of the assembly at the end of

the first pulse, but the nugget cannot be observed yet at this stage.



Fig. 1: Experiment facility used conducting the welding experiments; (a) Pedestal resistance spot welding machine, and (b) Signal monitoring and acquisition setup



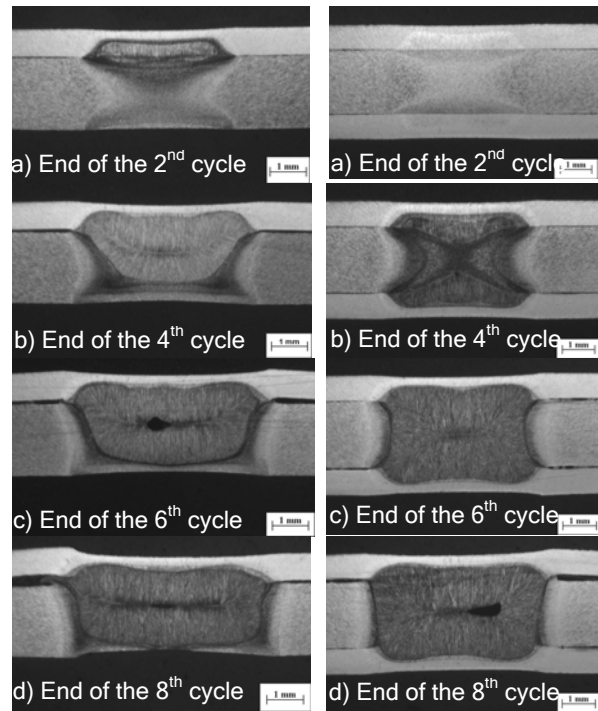
Case 1: Welding condition 400daN-11.2kA/4(6+2)-TH8
Case 2: Welding condition 450daN-10.6kA/4(6+2)-TH8

Fig. 2: Illustration of nugget formation of identical two- and three-sheet assembly of 2-mm thick AI-Killed Drawing Quality (AKDQ) steel sheet at the end of each pulse

For the latter pulses, the nugget penetration and development also show a trend similar to that of two-sheet assembly.

The macro-photographs of dissimilar sheet joining depicted in Fig.3 illustrate the nugget development at the end of each two cycles.

According to the welding standard with respecting to the sheet thickness presenting in the assembly, single pulse of eight cycles is selected for the welding operation. It is revealed from the nugget development kinetics at the end of the second cycle that the first hot zone still originates at the faying surfaces. The continuous growth of the nugget occurring in the assembly can be observed for the latter stages of welding.



Case 3: Welding condition 230daN-8.62kA/8Cycles-TH6
Case 4: Welding condition 230daN-7.36kA/8Cycles-TH6

Fig. 3: Illustration of nugget formation of two- and three-sheet assembly of 0,8-mm thick Interstitial Free (IF) and 2-mm thick AI-Killed Drawing Quality (AKDQ) steel sheet at the end of each two cycles

However, there is a slight development of the nugget in the thin gauge sheet for the latter stages of welding and the nugget develops more markedly in thicker sheet.

In case 4, two earlier hot zones start forming at the faying surfaces and the combination of these two hot zones takes place in the middle sheet as shown in Fig. 3b. The marked indentation can be observed at the surfaces of covering thin sheets as depicted in Fig. 3d for both cases.

To achieve the required surface quality standard, the relative deep indentation of the electrodes on sheet surfaces should be avoided. To reduce surface indentation for such assembly configuration, Schreiber⁵ proposed that different electrode cap profiles with the same face diameter should be used for joining assembly configuration with different sheet gauge.

In this section, different mechanisms of nugget formation in heavy gauge and stackup sheet joinings are reviewed on the basis of macro-metallurgical observation. However to investigate the other aspects concerning the relevant welding quality such as voids in the nugget, surface quality, shunt effect, electrode degradation, it may be more convenient to study only a typical sheet configuration recommended by the automobile manufacturer in order to reduce a large number of possible configurations.

The impact of electrical-thermal property variability on the weld geometry is studied for the case 1 by using FEA technique: (Case of joining sheet 2-mm thick AKDQ steel sheets with electrode TH8)

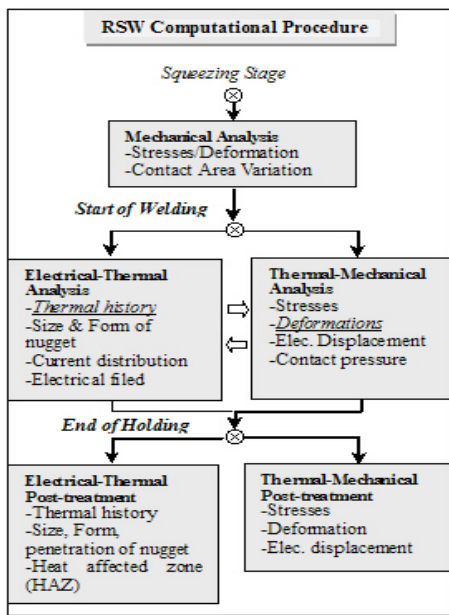


Fig. 4: Schematic illustration of computational procedure used in FEA technique⁴

3. THEORITICAL FRAMEWORK:

According to the axisymmetric and two-dimensional problem with fully coupling between the electrical and thermal phenomena, the coupling system governing equations are:

$$\rho \frac{\partial H}{\partial t} - \text{div}(\lambda \cdot \text{grad}T) - \text{grad}V \cdot \sigma \cdot \text{grad}V - Q = 0 \quad [1]$$

$$\text{div}(\sigma \cdot \text{grad}V) = 0 \quad [2]$$

where T, V are the temperature and the scalar electrical potential, respectively. ρ, λ and σ represent the density, the thermal conductivity and the electrical conductivity of the media and the temperature dependency characteristic can be taken into account. H is the enthalpy with temperature dependency. The

current circulation in electrical conductance creates the internal heat dissipation, which is generated by Joule heating effect represented in term of $\text{grad}V \cdot \sigma \cdot \text{grad}V$.

Three governing equations, namely, the compatibility condition, the constitutive relation, and the equilibrium equation in cylindrical coordinate are generally established for RSW thermal-mechanical analysis and can be found in the literature². The non-linear thermal elasto-plastic behavior is included and described by von-Mises criterion in this study.

To take into account the contact area variation manifesting in RSW process and produce more realistic model, the coupled thermal-electrical and thermal-mechanical is essential to be implemented. Furthermore, the coupled procedure allows the simulation of the process with a larger variety of electrode types and assembly configurations. The coupled procedure detail used in analysis is schematically presented in Fig.4.

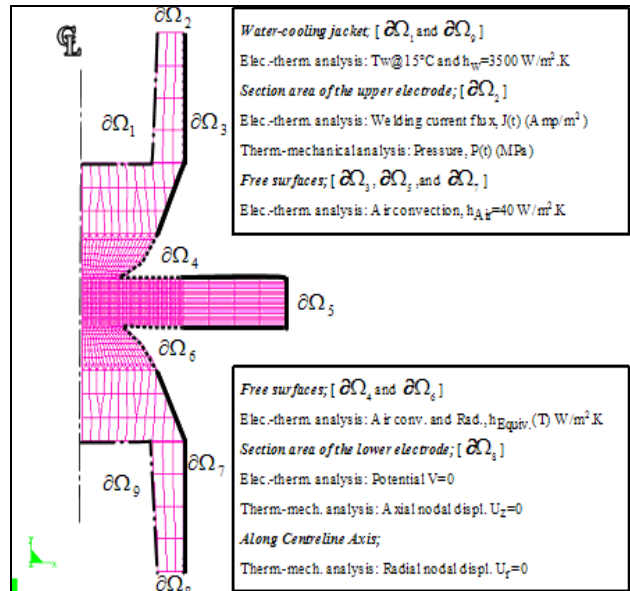


Fig.5: Structure/mesh construction and imposed boundary conditions of the electrical-thermal and thermal-mechanical computation with a meshing refinement in the high thermal, stress and deformation gradient regions

4. MESH CONSTRUCTION AND BOUNDARY CONDITIONS:

2-D axisymmetric models of two- as well as three-sheet joining with the application of curved-face electrode TH6 and TH8 are constructed.

Both electrical-thermal and mechanical contact elements are specially treated at the electrode-to-sheet and sheet-to-sheet interface. The imposed boundary conditions and representative mesh model can be found in Fig.5.

Prior to welding, the electrical initial conditions are set equal to zero, while the temperature of entire structure is maintained at temperature of 20°C. During the welding cycle, the welding current is applied at the top of the upper electrode and zero potential is imposed at the bottom surface of the lower electrode.

Consequently, the current flows from the upper electrode, passes through workpiece and terminates at the bottom annular section of the lower electrode. Both force and current are modeled from practical welding signals and defined as a time-dependent function.

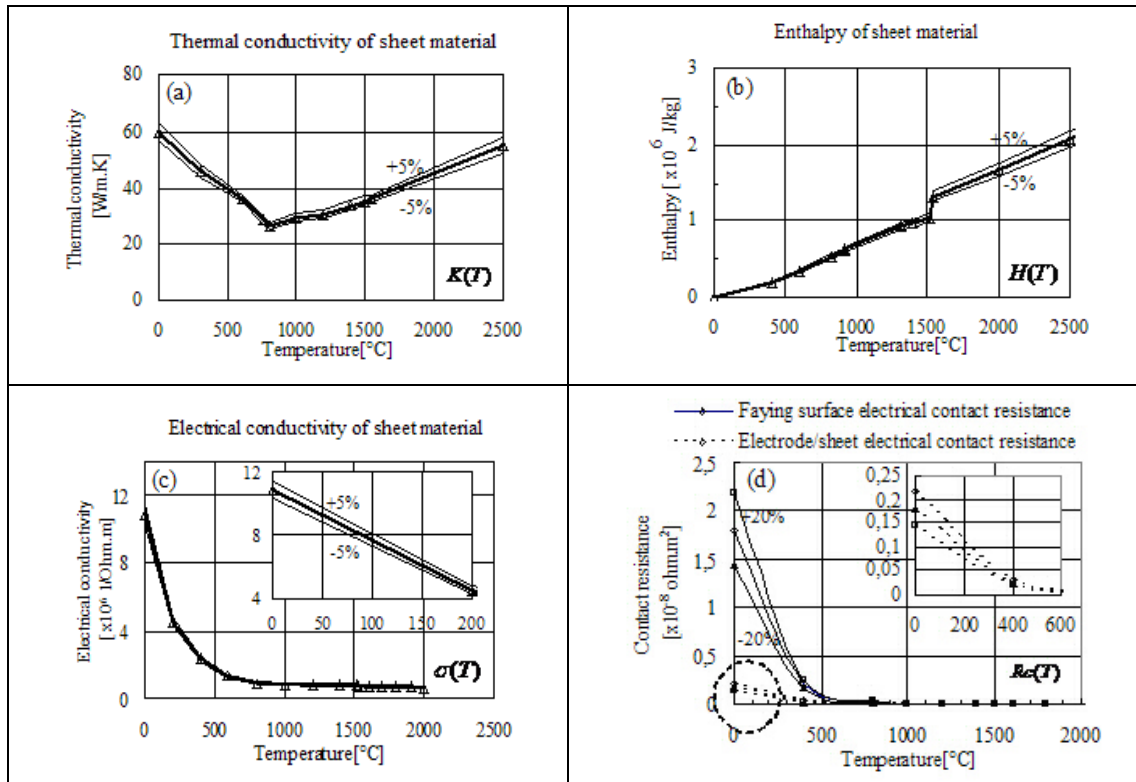


Fig. 6: Variability of electrical-thermal properties of sheet; (a) thermal conductivity extrapolated linearly after the fusion with variation of $\pm 5\%$, (b) enthalpy with variation of $\pm 5\%$, (c) electrical conductivity with variation of $\pm 5\%$, and (d) electrical contact resistance with variations of $\pm 5\%$ and $\pm 20\%$ [variation of $\pm 5\%$ is not displayed in Fig. 6d]

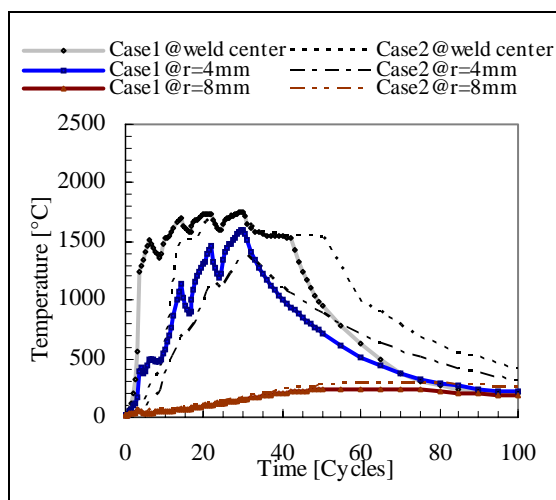


Fig. 7: Comparison between case 1 and 2 for radial thermal history experiencing along faying surface with the use of pulsed welding schedules

5. NUMERICAL SIMULATION RESULTS AND DISCUSSION:

Thermal history experiencing in two- and three-sheet joining cases illustrated in Fig.7

indicates that there is no variation in thermal history for the positions located far away from the nugget and the heat affected zone (HAZ), i.e. $r=8\text{mm}$., during the weld stage. Unfortunately for the sheet joining by RSW technique, it is not easy to attain the same value of the highest temperature in order to compare the thermal histories. This is due to the difference in the inherent welding parameters and the configuration used.

The drop of thermal history shows a similar trend to the four-pulsed current characteristic applied for welding operation, particularly in nugget region. However, the thermal history increases continuously for the region locating far away and it does not exhibit in similar manner to that experiencing in the nugget.

A comprehensive investigation for such thermal history characteristics associating with the supplementary post-heating pulse

welding schedule is also documented in Ref. 4.

5.1 IMPACT OF ELECTRICAL-THERMAL PROPERTIES ON WELD GEOMETRY:

The influence of electrical-thermal input data variability is studied through variations of $\pm 5\%$ of the property values in two-sheet configuration case as illustrated in Fig. 6. In this study the degree of variation for electrical contact resistance is brought up to $\pm 20\%$ since it is widely agreed that it has a strong impact on the nugget and HAZ development. Nugget and HAZ zones are defined by 1500°C and 730°C isothermal contours, respectively.

The influence of the electrical/thermal material property on the nugget and HAZ size and geometry is discussed. The summarized details of thermal-electrical property variation influencing weld geometry are shown in Fig. 8. It is disclosed from the variability of input property that the sheet electrical conductivity is the most significant input influencing on the weld geometry among other thermal parameters. The decrease in thermal

conductivity, enthalpy or electrical conductivity results in the enlargement of the weld geometry. Increasing electrical contact resistance also results in larger final nugget and HAZ geometry, but less significant influence comparing to those of other dominant thermal parameters.

Electrical contact resistance plays a great role on the weld geometry development at the early welding stage in comparing Fig. 9a and 9b. Considering the variability of -20% illustrated in Fig. 9a, the nugget does not appear yet at the end of the first pulse. However, the comparison of simulated final nugget found at the end of welding shows insignificant difference as depicted in Fig. 9b. The final nugget size validation of two-and three-sheet joining with TH8 electrode can be found in Fig. 10. In three-sheet joining case, the predicted results are also similar to those shown in the case of two-sheet joining that the simulated final nugget size is slightly smaller than that obtained from the welding experiment.

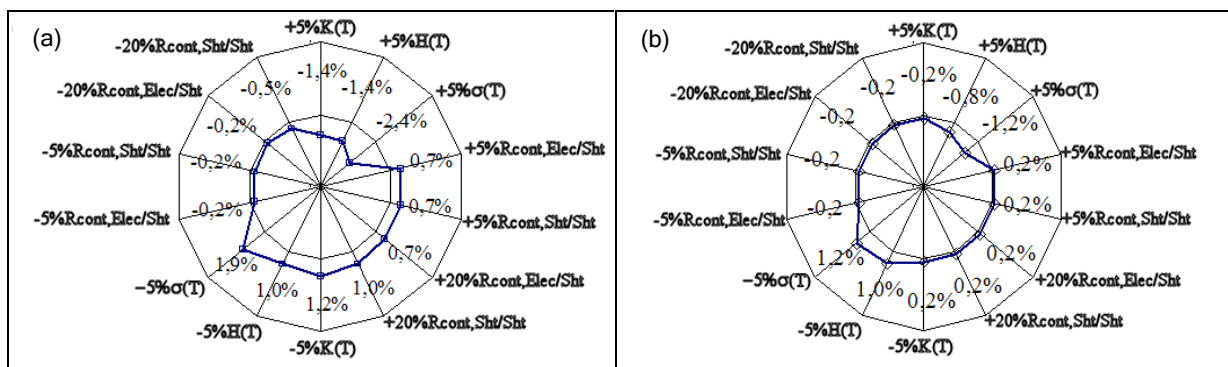


Fig. 8: Comparison of the relative variations in nugget and HAZ geometry at the end of welding due to $\pm 5\%$ variation of thermal-electrical properties and $\pm 20\%$ variation for the contact characteristics; (a) relative final nugget diameter size, and (b) relative final HAZ diameter measured at the faying surface

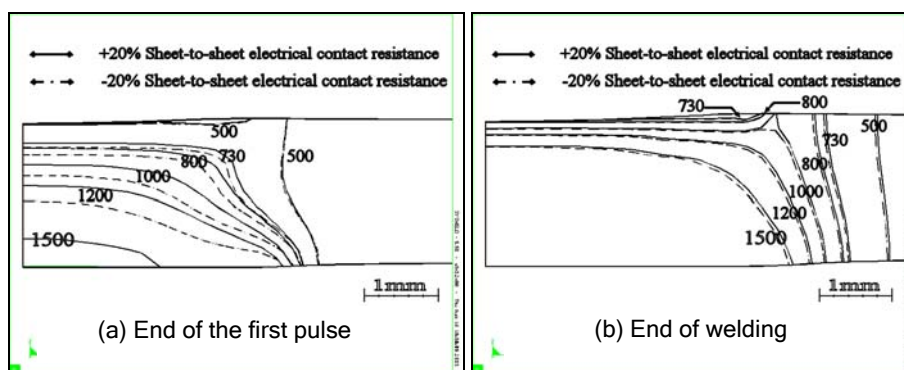


Fig. 9: Nugget and HAZ geometry due to $\pm 20\%$ variation for the faying surface electrical contact resistance (Case 1); (a) at the end of the first pulse, and (b) at the end of welding

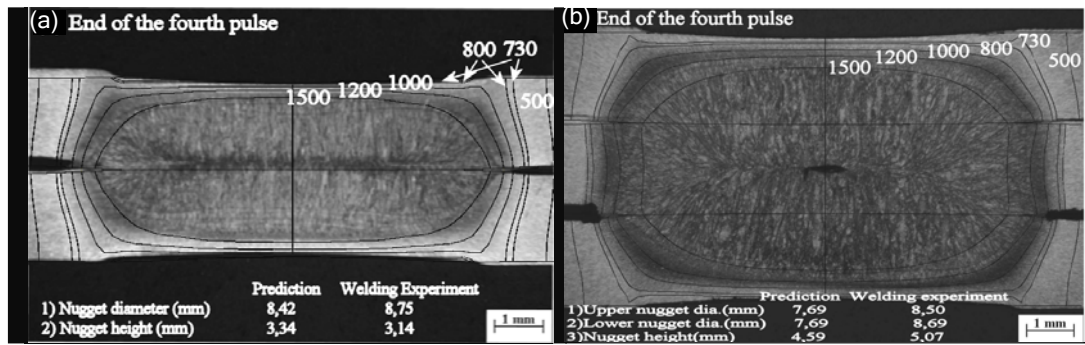


Fig. 10: Validation of final nugget and weld geometry for two-sheet and three-sheet joining of sheet material@2mm-thick AKDQ sheet grade at the upper weldability domain; (a) Final nugget geometry validation of case 1, and (b) Final nugget geometry validation of case 2

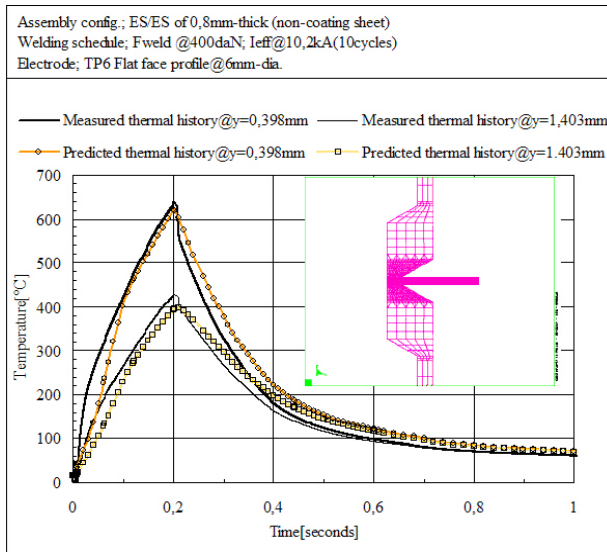


Fig. 11: Validation of thermal history experiencing at different positions in the lower electrode

5.2 THERMAL HISTORY MEASUREMENT AND VALIDATION:

To validate the thermal history of the RSW process, two micro-thermocouples are embedded at the positions of 0,398 and 1,403 mm away from the electrode face. For this joining case, single pulse schedule of ten welding cycles is applied for 0,8-mm thick of two AKDQ steel sheet joining.

The simulated thermal history in Fig.11 shows a good qualitative agreement with the experience for both heating and cooling stages. Higher heating rate is observed for the position locating near the electrode face. A slight discrepancy of the heating and cooling rates at the early stage of welding can be seen in the validated results.

6. CONCLUDING REMARKS:

A finite element analysis model with electrical-thermal and thermal-mechanical coupled procedure applied studying non-coating steel sheet joining by RSW technique is presented. The following conclusions can be drawn from these results:

i) It is found that a decrease in any one of three dominant properties being the thermal conductivity, the enthalpy or the bulk electrical conductivity of sheet results in the enlargement of the simulated nugget size.

The bulk electrical conductivity of sheet can be considered as a key input for both nugget and HAZ size variations. The faying surface contact resistance evolution has a significant role on the nugget development, particularly at the beginning of welding. The influence of electrode-to-sheet contact resistance shows a similar trend to that of faying surface contact resistance on the nugget development.

ii) Final nugget size and geometry validation shows a quantitative agreement for the final nugget size at the end of welding in case of two-sheet joining. The comparison between predicted and measured thermal history is in a good agreement for the magnitude of temperature. Only a slight discrepancy in heating and cooling rates is observed.

REFERENCES:

- [1]Srikunwong, C., Dupuy, T. and Bienvenu, Y.: "A Decoupled Electrical-Thermal and Mechanical Model for Resistance Spot Welding", *Proc. 15th ME-NETT seminar*, Nov., 2001, Vol.2, pp. 76-84.
- [2]Murakawa, H., Kimura, F., and Ueda, Y.: "Weldability Analysis of Spot Welding on Aluminium using FEM", *Mathematic Modelling of Weld Phenomena III*, Cerjak, H., and Bhadeshia, H.K.D.H., eds., 1997, pp. 944-966.
- [3]Gould, J.E.: "An Examination of Nugget Development during Spot Welding Using Both Experimental and Analytical Techniques", *Welding journal*, 65(1), 1987, pp. 1s-10s.
- [4]Srikunwong, C., Dupuy, T., and Bienvenu, Y.: "Numerical Simulation of Resistance Spot Welding Process using FEA Technique", *Proc. 13th International Conference on Computer Technology in Welding*, Siewert, T.A., ed., NIST and AWS, June 2003, Orlando, FL., pp. 53-64.
- [5]Schreiber, S.: "Investigations into Three-Member Welding", *Welding and Cutting*, 53(2001), No 11, E 252-E259.